Available online at www.sciencedirect.com

ScienceDirect

Procedia CIRP 113 (2022) 353–360

www.elsevier.com/locate/procedia

ISEM XXI

Electrophotographic Powder Application for Metal Powder bed based Additive Manufacturing

Julia Foerster[a,*], Krunoslav Vranjes[a], Maximilian Binder[a], Georg Schlick[a], Christian Seidel[a,b], Johannes Schilp[a,c]

a Fraunhofer Institute for Casting, Composite and Processing Technology IGCV, Augsburg
b University of Applied Sciences Munich, Department for Mechatronics and Applied Sciences, Munich
c University of Augsburg, Chair of Digital Manufacturing, Augsburg

* Corresponding author. Julia Foerster; Tel.: 0049 821 90 678 321; E-mail address: Julia.foerster@igcv.fraunhofer.de

Abstract

The scope of this paper is the systematic investigation and conceptual design of a process based on the principle of electrophotography for the application of particles on a build plate with the focus on powder bed based fusion of metals by means of a laser beam (PBF-LB/M). Using a translational prototype based on the stamp principle, influencing parameters for particle transfer from the photoconductor to the build plate are investigated. For this purpose, the process sequence is extended for the first time by the process step of powder deposition in comparison to [1, 2]. To reduce possible influences of the examination, the attraction of the powder to be deposited is performed without the exposure step of the photoconductor. The investigations of this work concentrate exclusively on a full-area attraction and its deposition. Significant parameters for the system are identified and measures to ensure a reproducible deposition are derived. Within the scope of experimental investigations, the PBF-LB/M typical powder 1.7147 (20MnCr5) with a particle size distribution of 15 to 56 µm is tested with regard to the deposition quality (surface coverage density and layer thickness) in a single- and multi-layer deposition. The stacking of the particle layers not only increases the area coverage density, but also demonstrates the basic transferability for generating a powder bed, which is required for additive manufacturing.

Keywords: Electrostatic; Deposition; Laser Beam Melting; Powder Recoating; Metal Powder; Additive Manufacturing; Organic Photoconductor, Powder Bed Fusion.

Nomenclature

ATT	Attraction
ABS	Acryl-Butadien-Styrol
c_E	Coefficient of proportionality of E_{DEP}
DEP	Deposition
DP	Deposition Plate
E-Field	Electrical Field
EL	Photoconductor´s Electrode
EP	Electrophotography
MV/m	Megavolt per meter
OPC	Organic Photoconductor
P	Potential
PB	Powder bed
PCD	Particle area coverage density
PSD	Particle size distribution
PBF-LB/M	Powder bed based fusion of metal with a laser beam,
V	Volt

1. Introduction

Powder bed fusion of metals with a laser beam (PBF-LB/M) belongs to the most relevant additive manufacturing processes in industry [3]. In PBF-LB/M, metal powder is selectively

2212-8271 © 2022 The Authors. Published by Elsevier B.V.

10.1016/j.procir.2022.09.142

melted by means of a laser. A core procedure within the process is the powder application, which is conventionally primarily contact-based, e.g. by means of a rake [4]. If multi-material powder application is needed, or the powder to be recoated is not sufficiently flowable [5], there are limitations in powder application. In that case a promising technology is the electrophotography (EP). EP is the basis of modern office laser printers; its powder application is based on the principle of the attraction of electrical charges. The powder attraction and deposition operates without contact. On first considerations, metallic powders seem physically contradictory to the way electrophotography works, due to the high electrical conductivity of metals.

In this paper, the application of a gas atomized steel powder is considered in on the basis of electrophotography with regard to function and deposition quality. To predict process-determining parameters, a physical model is derived from the forces required or to be overcome for deposition. A test rig has been developed for experimental qualification of the powder application. This was used to extend the electrophotographic process to include the deposition sequence. For this purpose, measures for stabilizing the process and for the targeted variation of the process-determining parameters are demonstrated. Based on the findings on single-layer deposits, multilayer deposits have been tested and quantified.

2. State of the Art of Electrophotographic Application of Metallic Powders in Additive Manufacturing

The conventional EP process follows six process sequences, which are also valid for AM:
1. charging of the photoconductor, 2. exposure of the photoconductor, 3. attraction of the particles, 4. deposition of the particles, 5. fixation of the particles and 6. cleaning and discharge of the photoconductor. For a more detailed description of the process steps and further information on the structure of a photoconductor, see [6–8]. As mentioned in [1], approaches in the research environment in which EP is used in powder bed based additive manufacturing, already exists.

Up to now, research activities have shown a particular challenge in the deposition sequence of metallic particles. KUMAR ET AL. observed oscillating particles in experiments on the processing of metal powders and therefore excluded them [9]. BOIVIE ET AL. developed the metal printing process for the first time. They were able to realize a powder application with pure metal alloys and ceramics by electrically insulating the powder-carrying components. The subsequent solidification of the powder layers was achieved by pressing and sintering [10, 11].

The ability of the electrophotographic process to produce a powder bed that is also suitable for other metal-based AM processes, in particular for PBF-LB/M is still unclear. Equally unclear is the investigation of process-determining parameters and their effect on the deposition quality. First investigations on the transferability of the essential EP process sequences into PBF-LB/M have been explained in [1, 2, 12, 13] with the focus on the application of the PBF-LB/M typical powder of 1.7147 (20MnCr5) with a PSD of 15 – 56 µm, as this is a gas atomized steel powder, which is widely used in PBF-LB/M. The focus was on charging an organic photoconductor (OPC) under ambient machine conditions [1, 12] as well as initial investigations on powder attraction [2, 12]. OPCs are the most widely used and technically developed materials in EP [7]. Due to the moderate ambient temperature of a maximum of 60 °C in the build chamber of a PBF-LB/M machine [14], they are considered suitable for powder processing with regard to the environmental conditions. The investigations in this paper continue the work of [1, 2, 12, 13]. In case of a full-area deposition, no exposure of the imaging (laser) unit takes place, which means that the process window for attraction and deposition can be directly related to the maximum area of the OPC.

3. Physical System Modeling and Experimental Setup

In the case of powder application by electrophotography, the following subsystems and their interactions typically occur:

- Particles in the ambient medium among each other or to the respective surfaces of the components; forces of adhesion and cohesion between spheres or between a sphere and the surface (e. g. capillary forces, Van der Waals forces, Brownian motions, image forces, etc.)
- Particles in the gravitational field of the earth (e.g. weight force, buoyancy force, etc.)
- Particles in the electric field between the charged photoconductor and the attraction or deposition plate (e.g. Coulomb force, electric field force, etc.)

Further interactions result from the involved surfaces and their material-specific properties, such as density, electrical conductivity and morphology, etc.

On the one hand approaches for the mathematical calculation of the necessary field force have been investigated under consideration of the particle mass and size [9, 15, 16]. In idealized form, the weight force of individual particles is already taken into account for particle attraction and deposition in addition to the electric field force. As an extension to this, it is assumed that detaching forces support the electric field force in depositing particles. The adhesive and cohesive forces, on the other hand, must first be overcome by the electric field force. For the approximation of statements on particle behavior, the Coulomb and electric field forces are of particular importance in this work [17]. From [17] it can be seen that there is an adhesive relationship between the van der Waals forces and the weight force. Especially for particles with a diameter under 100 µm as used in AM, the van der Waals forces dominate and have to be overcome by the electric field force.

The constellation when the photoconductor is positioned above the powder bed or the building plate can be idealized as a plate capacitor; the photoconductor and the attraction or deposition plate each form a capacitor plate. The field lines between the photoconductor and the powder bed or deposition plate are considered homogeneous and therefore equidistant [2, 18, 19]. The potentials of these surfaces will be used in the estimation of electric field strengths throughout this work.

Fig. 1 shows a schematic illustration of the charge distribution within the OPC during a powder deposition, which is generated from a full-area particle attraction at the OPC. A central effect is the electrostatic induction (electrical influence). This results from displacements of the freely moving charges under the influence of an accumulation of charge (source charge). The

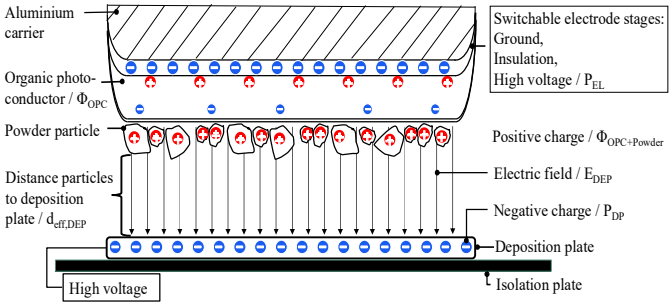

Fig. 1: Schematic system modeling for charge distribution during deposition of metallic powder in the electrophotographic process in analogy to a plate capacitor.

generated or resulting charge is always inverse to the source charge [20]. The particles used in this work are assumed to be ideally conductive in the model. Thus, it can be assumed that the voltage for attraction and deposition, which is applied to the plate, reaches the uppermost particle layer unhindered within the powder bed. The ability to distribute charge thus results from free exchange of charge between the particles and the source charge of the attraction or deposition plate. In the case of electrical conductors, the charge concentration in the contact area is greater than in the case of non-conductors, since the charge carriers are freely mobile on the surface. This means that their electrostatic attraction is also greater due to the contact potential. In order to introduce a charge in a targeted manner or to prevent the metallic particles from discharging, the attraction and/or deposition plate is considered to be isolated from the environment.

Of particular importance is the contacting of the photoconductor´s electrode (EL) as indicated in Fig. 1. This can be switched and set to the following four discrete states: Ground, insulation, voltage positive and voltage negative. If the electrode is grounded, an exchange of charge carriers – as it is necessary, for example, during exposure – is supported; in the insulated state, the exchange of charge carriers is eliminated in order to minimize a charge decay, e.g. during transport. To increase the deposition quality, the voltage provided is intended to specifically influence the external field on the photoconductor or to release the adhering particles for deposition.

An OPC is optimized for the negative charge. Thus, the necessity of the positive charge of the powder bed arises. With the attraction of the positive particles on the photoconductor, the negative voltage on the deposit plate follows. When the positively charged powder particles come into contact with the negative charges on the surface of the OPC, a charge equalization takes place. Thus, the charge of the attracted particles is lowered and the surface of the OPC is positively charged after the charge equalization corresponding to the particles. Due to the positive surface of the OPC and in case of the grounded EL, electrons are therefore transported as shown in Fig. 1 (EL stage I Ground). This creates an electric field (E-Field) in the OPC between the electrode and the particles. Since the particles are positively charged, their tendency is to migrate toward the electrode. This generates an additional force against which the E-Field between the deposition surface and the particles must act.

For the investigation of the process, the generated electric field strength, as well as the voltages or potentials at the photoconductor or the deposition plate are in focus. The physical relationship (from capacitor fields) with the voltage (U) and the distance (d) of the capacitor plates to the field strength (E) can be used to provide a mathematical approximation of the observable particle movement during deposition.

$$E = \frac{U}{d} = \frac{\Phi_{OPC+Powde} + |P_{DP}|}{d_{eff,DEP}} \quad (1)$$

The capacitor equation (1) is adapted to the conditions of the electrophotographic process. The effective distance between the upper particle layer on the OPC and the deposition plate ($d_{eff, DEP}$) as well as, in the present two-dimensional consideration, the added amount of the stresses between the OPC with attracted powder ($\Phi_{OPC+Powder}$) and the deposition plate (P_{DP}) have to be considered.

For the qualification of the deposition of metallic particles by electrostatic field forces an experimental test setup was developed. The test setup is described in detail in [1, 2] and is shown in Fig. 2. The maximum accuracy of the movement system of 0.3 mm was considered sufficient to describe the initial feasibility of metal powder deposition for PBF-LB/M. All components under voltage (see Fig. 2 voltage signs) were isolated from the rest of the test setup. An electrostatic field measurement sensor (Keyence SK-050) in the near-field mode with a measurement distance of 16 mm was used to measure the surface potential on the photoconductor. Measurements were taken at different times in the process. They provided information about the resulting surface potential on the photoconductor after charging (Φ_{OPC}), after powder attraction ($\Phi_{OPC+Powder}$) and after powder deposition ($\Phi_{OPC-Powder}$). The individual measured values were used, in particular, for process control to determine a process window for reproducible deposition.

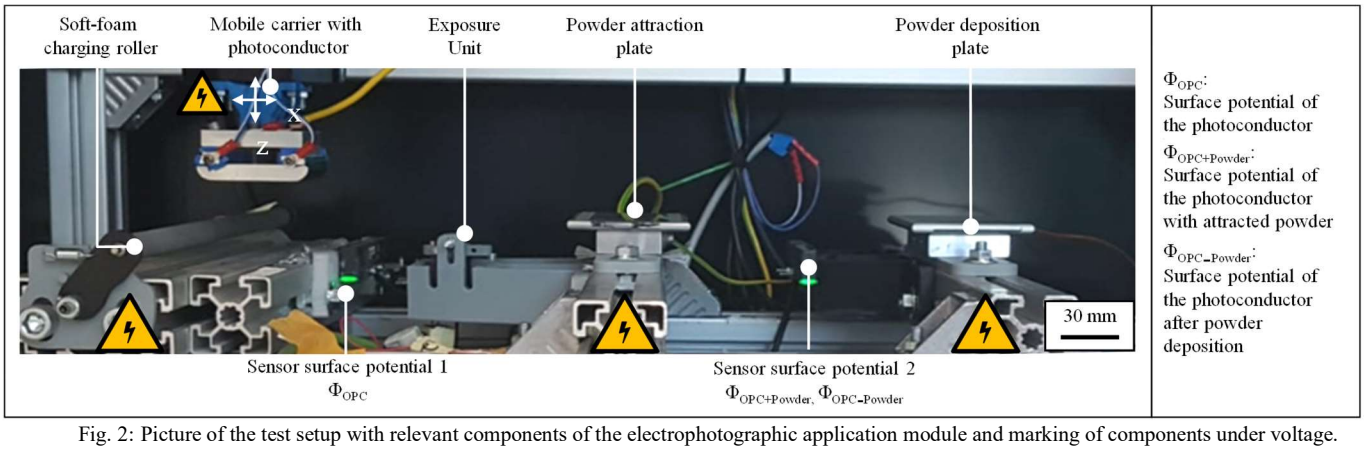

Fig. 2: Picture of the test setup with relevant components of the electrophotographic application module and marking of components under voltage.

4. Single-Layer Application of Metallic Particles

To qualitatively evaluate the effects of the process parameters on the deposition during the test series, the deposition quality is classified into six categories. The classification is carried out visually in accordance with the criteria in Tab. 1.

Table 1. Categories for the qualitative evaluation of powder deposition for single-layers.

Category	Description
A	Full-area, homogeneous and optically dense layer
B	Full-area, homogeneous and optically not dense layer
C	Full-area and non-homogeneous layer
D	Partial-area and homogeneous layer
E	Partial-area and non-homogeneous layer
F	No layer visible

Based on the test setup, experiments on deposition were carried out and parameters relevant to the system were determined in order to generate single-layer deposition. The individual experimental steps were defined by the following modules:

(1) Contact charging device, which consisted of a soft-foam contact roller. The charging procedure induces the time-dependent surface charge parameter (Φ_{OPC}) on the OPC´s usable surface (50x50 mm^2). For particle attraction, the surface of the photoconductor was charged to a specific potential with a tolerance of ±50 V. The measured value was used to monitor the specified potential Φ_{OPC}.

(2) The powder attraction plate was realized as an isolated aluminum plate connected to the HV source, which directly sets the potential (P_{PB}) on the plate's top surface. The powder was applied to the plate with a layer thickness of 550 µm by a film applicator from BYK-Gardner. To achieve a constant E-Field, depending on Φ_{OPC}, the voltage on the powder bed was controlled accordingly. The effective distance to the attraction ($d_{eff, ATT}$) was constantly set to 0.8 mm. Immediately after attraction, the EL was switched to the insulated state to minimize potential decrease due to charge exchange.

A full-area attraction was observed for the 1.7147 powder from an E-Field (E_{ATT}) of approx. 0.7 MV/m to approx. 1.4 MV/m [2] and formed the starting point of the test series for powder deposition. Thereby, $P_{PB} > \Phi_{OPC}$ was always set. An increase of the E-Field for attraction led to an optically denser layer. When the voltages or the E-Field were increased further, flashovers occurred, which resulted in damage to the OPC and necessitated replacement. At voltages leading to a lower E-Field, only partial area attraction of lower quality was observed.

(3) The deposition plate design was the same as for the attraction plate. The process of deposition started with the measurement of the potential of the attracted particles at the OPC ($\Phi_{OPC+Powder}$). Right before the photoconductor moved down to the deposition plate, the electrode of the OPC was switched to the respective state. The distance to the deposition plate ($d_{eff,DEP}$) was also 0.8 mm. After deposition, the measurement point $\Phi_{OPC-Powder}$ indicated the potential present at the photoconductor.

(4) The process of deposition was completed with the camera image of the powder deposition on the plate.

(5) Cleaning and discharging of the photoconductor was performed manually using ethanol and a cloth.

4.1. Impacting the photoconductor´s electrode for particle deposition

The initial approach was to increase the E-Field for deposition. It is assumed that a high E-Field leads to a fully dense deposit. For this purpose, test series for deposition with increase of E_{DEP} were carried out with control of the EL to ground and to insulation, respectively. The voltage of the deposition plate (P_{DP}) was formed via the predetermination of the target E_{DEP} by using equation (1) and is thus directly dependent on the value $\Phi_{OPC+Powder}$. Fig. 3 shows a direct comparison of selected powder deposits.

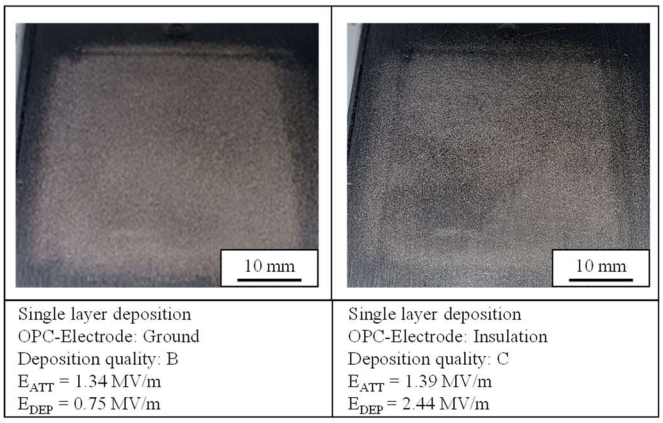

Fig. 3: Selected images of full-area single-layer depositions under impact on the photoconductor electrode: Ground (left), Insulation (right). Legend: E_{ATT}: Estimation of the electric field of the attraction, E_{DEP}: Estimation of the electric field of the deposition.

It can be seen that full-area deposition was possible in both test series. In the case of the deposition with insulated electrode, on the one hand only partial deposition was possible and on the other a clear edge around the deposition was observed. The highest achievable deposition quality was C. It should be noted that the E-Field was higher by a factor of approx. three compared to the deposition without grounded electrode. This may be due to the fact that the eliminated charge exchange leads to an irregular field. Thus, the defects would be due to an insufficient field and the deposit over the edge due to field peaks. The best quality was category B, achieved by utilizing a grounded electrode .

Tab. 2 shows an overview of relevant measured values and correlations from the test series for deposition with grounded EL. Increasing or decreasing relations of the measured values leading to a deposition quality less than B is indicated by an arrow, if the value has a difference of more than 20 V. This difference corresponds to the measurement inaccuracy of the E-Field sensors. The measured values of the surface potentials are highlighted in bold. The measuring point Φ_{OPC} was almost constant due to the specified tolerance band in the process control.

Table 2. Process parameters and measured values of the surface potentials on the photoconductor for the test series with grounded photoconductor electrode in relation to the deposition quality B.
Legend: Φ_{OPC}: Surface potential of the photoconductor
P_{PB}: Potential of the powder bed
E_{ATT}: Estimation of the electric field of the attraction
$\Phi_{OPC+Powder}$: Surface potential of the photoconductor with attracted powder
E_{DEP}: Estimation of the electric field of the deposition
P_{DEP}: Potential of the deposition plate
$\Phi_{OPC-Powder}$: Surface potential of the photoconductor after powder deposition
Bolt marked values represents measured surface potentials.

Process parameters and measured values	Quality of the depositions				
	B	C	D	E	F
Φ_{OPC} in V	**-382**	**-365**	**-372**	**-374**	**-375**
P_{PB} in V	692	710	702	700	710
E_{ATT} in MV/m	1.34	1.34	1.34	1.34	1.35
$\Phi_{OPC+Powder}$ in V	**273**	**261**	**301↑**	**322↑**	**357↑**
P_{DP} in V	-328	-402↑	-337	-397↑	-279↓
E_{DEP} in MV/m	0.75	0.83↑	0.75	0.9↑	0.78
$\Phi_{OPC-Powder}$ in V	**-57**	**-54**	**-62**	**-92↓**	**-85↓**

The following parameters were kept constant in the test series:
Voltage at the charging roller = -700 V,
Target value of the Φ_{OPC} = -375 V, $d_{eff, ATT}$ = 0.8 mm, $d_{eff, DEP}$ = 0.8 mm,
Attraction and deposition duration = 2 s.

It is recognized that the constant charge and attraction parameters results in different values of $\Phi_{OPC+Powder}$. Possible influencing factors on this surface potential are, the voltages or the potential of the photoconductor at the charge roller and at the powder bed, the distance between OPC and the PB, and also the dwell duration for attraction. Since these factors were kept constant in the series of experiments, the variation in the value so far cannot be explained solely by these factors. However, it is evident that the deposition quality decreases as the $\Phi_{OPC+powder}$ increases and the lower the difference to the controlled P_{DP} becomes.

Due to the non-constant value of the surface potenzial of the OPC with attracted powder, no constant value can be specified for the actual E-Field. It should be noted that a high electric field does not per se lead to better deposition. One possible interpretation of the measurement results is that the deposition quality depends on a certain ratio of the surface potenzial of the OPC with attracted powder to the potential of the deposition plate, following $P_{DP} > \Phi_{OPC+Powder}$.

An indicator of deposition quality seems to be represented by the remaining value of the surface potential of the photoconductor after the powder deposition

4.2. Charge Stabilization of the Potential at the Photoconductor

From the investigations on the process window with grounded EL, it can be seen that the measured value $\Phi_{OPC+Powder}$, despite the same process parameters of Φ_{OPC} and P_{PB}, is subject to certain fluctuations in the quantity, which have a negative effect on the deposition quality. Since this measured value ends the process sequence of attraction and passes into the process sequence of deposition, it is of importance for the stability and reproducibility of the overall process. Further influences are suspected in charge exchange processes between the particles and the OPC as well as between the particles and the ambient medium. Thus, a decrease in potential, e.g. during transport times, can have an appreciable influence. Immediately after the powder is attracted, charges are exchanged between the OPC and the particles due to the contact potential. However, due to the insulation of the OPC, the mutual exchange of charges is only possible to a limited extent.

Since the powder at the measured potential $\Phi_{OPC+Powder}$ is already located at the OPC and thus cannot be subsequently charged via the contact charge, e.g. via a positive charge roller, a contactless particle charge is investigated with a corona unit of the sharp MX type. The corona unit is operated with a positive voltage, whichis expected to move the positive charges on the particles towards the negative potential of the photoconductor due to repulsion. The negative charges on the photoconductor should in turn be attracted to the particles. Thus, a rapid charge exchange is expected.

Fig. 4 shows exemplary curves of the measured values of $\Phi_{OPC+Powder}$ as an average of 10 individual measurements of the surface potential on the OPC with attracted powder.

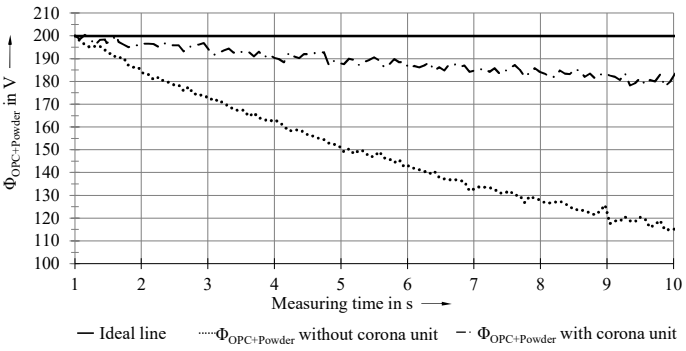

Fig. 4: Potential decrease at the photoconductor with attracted powder with and without additional charging through corona unit compared to the ideal, loss-free surface potential.
Legend: $\Phi_{OPC+Powder}$: Surface potential of the photoconductor with attracted powder

The dotted graph represents the potential drop without additional charging by means of the corona unit. The average standard deviation is 26.13 V (17 %). The charge drop in relation to the ideal, loss-free potential curve is approx. 42 % respectively 85 ± 26,12 V after 10 sec.

The photoconductor with the attracted powder passes over the corona unit three times at a distance of approx. 1 mm, and a voltage of 1,200 V is applied to its wire. The potential decrease within the measurement period after the OPC has been moved across the corona unit (measured values $\Phi_{OPC+Powder+Corona\ unit}$) is only about 10 %, respectively 20 ± 6,05 V (Fig. 4, dot-dash graph). The average standard deviation is 6.05 V (3 %). First improvements could be observed from $P_{Corona\ unit}$ = 800 V. 1,200 V represent the maximum voltage in the experimental setup.

This shows that charge stabilization by means of corona unit results in a more stable potential curve and rapid charge equalization of the powder with the OPC. Unchanged was the non-constant initial value of the potential with which the measurement position $\Phi_{OPC+Powder}$ is reached. Furthermore, no significant increase in the quantity of $\Phi_{OPC+Powder+Corona\ unit}$ could be

achieved at the maximum voltage values of the corona unit compared to $\Phi_{OPC+Powder}$. Thus, the deposition quality cannot be controlled by a corona unit only. However, with additional use of the corona unit, the potential of the particles was significantly stabilized over the transportation time.

4.3. Optimization of the Deposition quality

In the following experiments only deposits were considered, where a quantity of $\Phi_{OPC+Powder}$ was in the interval from min. 200 V to max. 275 V. In addition, charge stabilization with the corona unit and a voltage of 1,200 V was always utilized.

In accordance with the forces in the physical system model, it is assumed that a ratio of the surface potential at the photoconductor with attracted powder to the deposition plate´s voltage correlates with the E-Field for the deposition and therefore with the deposition quality. For this purpose, a proportionality coefficient (c_E) is introduced as shown in equation 2.

$$c_E = \frac{P_{DP}}{\Phi_{OPC+Powder}} \quad (2)$$

c_E is used to adjust the P_{DP} depending on the potential of the particles on the photoconductor in such a way that a constant ratio to the deposition of the particles can always be maintained. The polarities of the potentials are always opposite to each other; $\Phi_{OPC+Powder}$ is positive and P_{DP} is negative. A process window can be derived by means of an empirical determination of c_E in which reproducible and stable deposition should be possible.

Fig. 5 contains the measured values of all measuring positions, the voltages at the deposition plate and the quality of the depositions as a function of c_E. Plotted and evaluated are test runs where the measured value $\Phi_{OPC+Powder}$ was min. 200 V. The measurement points $\Phi_{OPC+Powder}$ and $\Phi_{OPC+Powder+Corona\ unit}$ are therefore almost constant and parallel to each other.

It can be observed that the measuring point $\Phi_{OPC-Powder}$ has a steadily decreasing potential. The course follows the P_{DP}; however, it is always lower in value. A deposit of at least quality B is produced when the c_E of 0.7 to 1.5 is reached. The two vertical arrows in Fig. 5 mark the beginning and the end of this deposition quality range, accordingly. In this case, the value of $\Phi_{OPC-Powder}$ results in potentials from about 0 V to about -180 V. For the deposit with the c_E of 0.7, the adhesion forces were sufficiently overcome. For a c_E between 1.2 and 1.3, a deposition quality of A was achieved. In this case, P_{DP} is only slightly higher than $\Phi_{OPC+Powder}$. With increasing c_E, the deposition quality decreases. An explanation is suspected in a too strong E-field. On the one hand, particles could be strongly accelerated and as a consequence of high kinetic energy hit the deposition plate in an undirected way. On the other hand, local field peaks could be induced, which act as centers of powder dislocations.

With the contacting of the electrode to the ground, an increase in the particle coverage density was realized. Furthermore, a voltage provided to the electrode should lead to the repulsion of the particles from the photoconductor and, as a result, to a further improvement in the deposition quality. Fig. 6 shows a direct comparison of selected powder deposits, which were produced with a positive voltage (left) and with a negative voltage on the EL (right).

In both test series, the area of the photoconductor can be seen. With the operation of the positive voltage, the particles are primarily found in the edge regions of the deposition area. It stands to reason that strong repulsive forces are acting in the E-Field to the sides. Following the system model for the influence and polarization, this can be estimated, for example, by a repolarization of the particles so that they are now also negatively charged. As a result, they repel from the negatively charged DP along the field lines bent to the edges.

In contrast, a negative voltage applied to the EL shows an optically dense, full-area deposition of category A and leads to a significant increase in quality. When a negative voltage is applied to the electrode, an electrical induction is created between the electrode and the particles located at the photoconductor. The positive charges on the particles will move to the surface towards the electrode, and the negative charges towards the deposition plate. This would increase the forces holding the particles to the surface. However, the carrier moves toward the

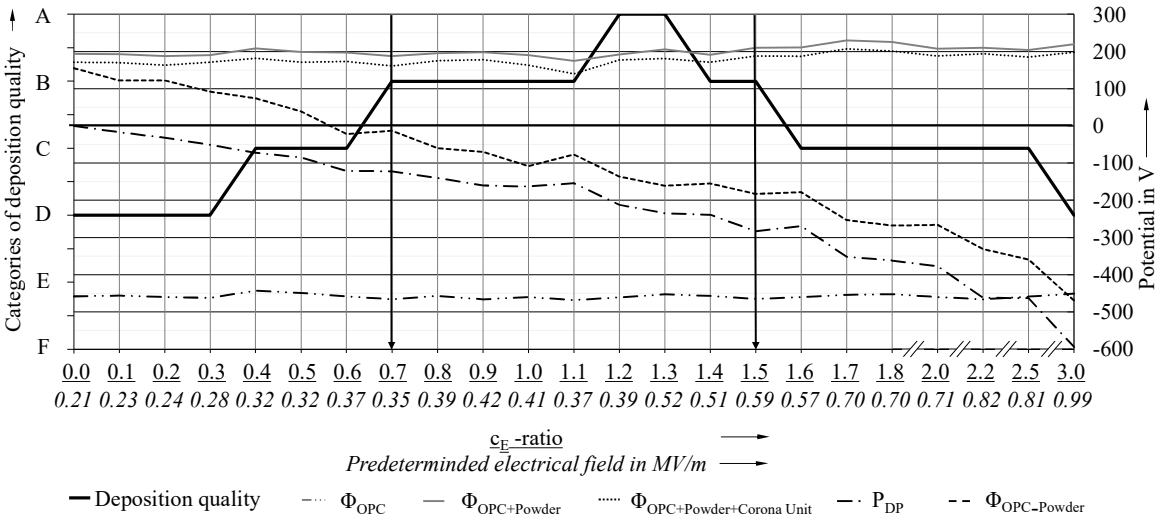

Fig. 5: Deposition quality and potentials during the deposition sequence as a function of the predetermined electrical fields and c_E-ratio.
Legend: cE: Proportionality coefficient for deposition, Φ_{OPC}: Surface potential of the photoconductor, $\Phi_{OPC+Powder}$: Surface potential of the photoconductor with attracted powder; $\Phi_{OPC+Powder+Corona\ unit}$: Surface potential of the photoconductor with attracted powder with the utilization of a corona unit; P_{DEP}: Potential of the deposition plate, $\Phi_{OPC-Powder}$: Surface potential of the photoconductor after powder deposition

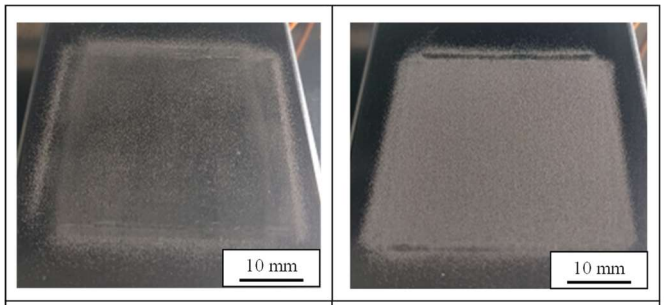

Fig. 6: Selected images of full-area single-layer depositions under the impact of EL: potential +120 V (left), potential -120 V (right).
Legend: E_{ATT}: Estimation of the electric field of the attraction,
E_{DEP}: Estimation of the electric field of the deposition.
cE: Proportionality coefficient for deposition

deposition plate, which is also negatively charged. It is assumed that as the photoconductor approaches the deposition plate with the negative potential, an interaction between the particles with the new, stronger potential of the deposition plate dominates. The negative charges, which had previously moved towards the deposition plate because of the voltage on the electrode, turn towards the weaker P_{EL}. The same happens with the positive charges on the particle surface.

The deposition with the quality of category A was analyzed with a laser microscope of the type Keyence VK-9710. The area covered by the particles (PCD) was determined in % in relation to the reference surface of the deposition plate. For this single-layer deposition of quality A, the PCD is 30.45 %. A layer thickness of 48 µm could be determined with the laser microscope measurement.

4.4. Investigation of the Particle Size Distributions

It can be observed that particles still adhere to the OPC after deposition. In accordance with the assumption that the van der Waals forces are dominant in this state, it should be possible to deposit particles larger than 10 µm from the OPC by electrostatic forces. To test this assumption, the PSD was measured on the basis of powder samples from the powder bed, from the OPC and from the deposition plate. The PSD was measured using laser diffractometry device from Malvern with the Mastersizer 3000. To take the samples, the process was stopped at the respective times and the powder was removed from the surfaces using a rubber spatula. Due to the small amount of powder per sampling, five samples were collected and measured together in the dispersing medium of deionized water. This resulted in an average of the individual samples. The particle size distributions determined were summarized in the usual PSD data with regard to the distributions at D_{10}, D_{50} and D_{90} in Tab. 3.

The analysis of the particle size distribution of the powder from the powder bed serves as a reference and confirms the PSD given by the powder manufacturer with approx. 15 - 56 µm. Starting from the powder that was attracted, the number of small particles present decreases over the application sequences – consequently the number of larger particles – attracted by the OPC increased (see Tab. 3).

Table 3. Results of the measurements on particle size distribution.

Mean values for distribution at	Powder from powder bed	Attracted powder from OPC	Powder from deposition plate
D_{10} in µm	13.33 ±0.11	18.10 ±0.53	22.17 ±0.12
D_{50} in µm	32.23 ±0.25	34.13 ±0.45	37.43 ±0.17
D_{90} in µm	56.70 ±0.30	58.30 ±3.07	62.47 ±0.28

This can be seen especially in the powder, which is on the deposition plate. It can be seen that hardly any particles smaller than 10 µm can be found in the deposition layer. These results confirm the assumption that larger particles tend to be attracted and deposited while particles smaller than 10 µm remain on the OPC. It is assumed that the adhesion between particles and the OPC is so strong that they remain attached to the photoconductor and cannot be detached by the E-Field acting on the particles.

5. Multi-Layer Application of Metallic Particles

In order to increase the particle coverage density and especially to verify the transferability of the electrophotographic powder application for the layer-by-layer build-up process of additive manufacturing, the stacking of individual layers to form multi-layer deposits was investigated. Single-layers were deposited on top of each other by varying the c_E and the voltage on the EL. After each deposition, the photoconductor was manually cleaned to remove residual particles. The distance between the OPC and the DP was kept constant at 0.8 mm for the multi-layer depositions. This increases the effective field force by reducing the distance as a result of an increasing particle layer. Fig. 7 shows full-area deposition stacks with the respective voltage values in comparison of the impact on the EL.

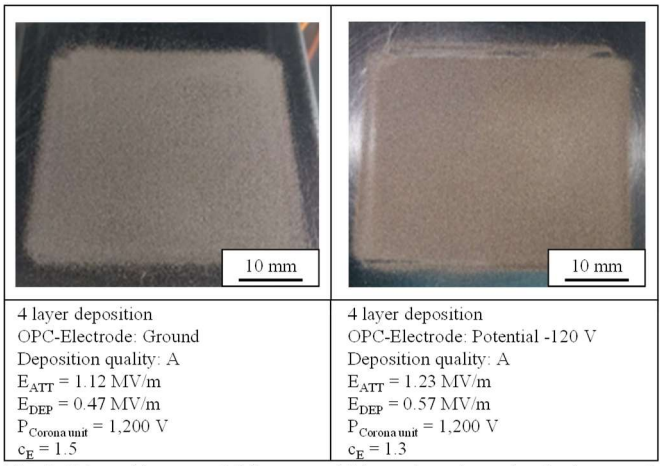

Fig. 7: Selected images of full-area multi-layer deposits under the impact of EL: Ground (left), Potential -120 V (right).
Legend: E_{ATT}: Estimation of the electric field of the attraction,
E_{DEP}: Estimation of the electric field of the deposition.
cE: Proportionality coefficient for deposition

The resulting PCD could be increased from 15 % for a single-layer deposition to over 63 % after only four depositions. With the voltage on the EL (P_{EL}) of -120 V, 95 % PCD was achieved after four depositions. With this 4-layer deposition with additional P_{EL} (see Fig.7 right), a total layer height of 68 µm was determined. In particular, particles with small diameters can first fill the spaces between the surface and in the

powder layers. As a result, the layer initially becomes denser and the height growth is lower.

When stacking the layers with additional P_{EL} of -120 V, displaced particle accumulations can be seen in the edge regions of the area (see Fig. 7 right). These may be due to an inhomogeneous field peaks between the geometric edge of the photoconductor and the deposition plate. Particles in this area follow the curved field lines and converge on the deposition plate in an offset manner.

Based on the 4-layer deposition stacking with additional P_{EL} of -120 V, a deposition of 20 layers was performed. This was generated with a P_{EL} of -120 V and the c_E control with 1.2. The PCD of the 20-layer deposit was 100 % and reached a total layer height of 124 µm. With further layers, it was observed that the deposited powder bed was shifted to the edge regions of the deposition area as a result of the increasing layer due to the rising E-Field.

6. Conclusion and Outlook

With the developed electrophotographic process, single layers for the powder material 1.7147 (20MnCr5) with a PSD of 15–56 µm have been reproducibly achieved with a homogeneously distributed particle coverage density of up to 30 % and a layer thickness of up to 48 µm. In the future, especially with regard to homogeneity, a comparison with conventional recoating mechanisms should be performed.

Under the impact of EL (grounding, insulation and P_{EL}) and by considering the ratio of $\Phi_{OPC+Powder}$ to P_{DP} (c_E), the quality of the deposited powder layer can be significantly increased. Indicators of an unstable process are fluctuating measured values of $\Phi_{OPC+Powder}$ and $\Phi_{OPC\text{-}Powder}$. In particular, the reproducibility of $\Phi_{OPC+Powder}$ requires further research in the future.

Based on the findings of reproducible single-layer deposition, layer-by-layer stacking of particles on the deposition plate was carried out. It can be shown that the quality of deposition in terms of homogeneity and areal density can be achieved to about 95 % and a layer thickness of 68 µm starting from four layers. When depositing 20 layers, a total layer thickness of 124 µm was achieved. In the future, an adaptation of the effective distance as a result of the increasing layer has to be considered. With the stacking of single-layers to form a multi-layer deposit, proof of the principle transferability of the mechanism for the additive manufacturing process has been provided.

Acknowledgments

The authors express their sincere thanks to the State of Bavaria and its Bavarian Ministry of Economic Affairs, Regional Development and Energy StMWi for funding the project Multimaterial Center Augsburg.

References

[1] Foerster, J.; Michatz, M.; Anstaett, C. et al.: Aspects of Developing a Powder Application Module based on Electrophotography for Additive Powder Bed based Processes. Machining Innovations Conference for Aerospace Industry (2020), p. 147–152.

[2] Foerster, J.; Michatz, M.; Binder, M. et al.: Electrostatic powder attraction for the development of a novel recoating system for metal powder bed-based additive manufacturing. Journal of Electrostatics (2021).

[3] Wohlers, T. e. A.: Wohlers Report. 3D Printing and Additive Manufacturing. WOHLERS ASSOCIATES, INC.

[4] Gebhardt, A.: Generative Fertigungsverfahren. Hanser Verlag (2013), p. 59 - 66, p. 66- 68.

[5] Girnth, S.; Koopmann, J.; Klawitter, G. et al.: 3D hybrid-material processing in selective laser melting: implementation of a selective coating system. Progress in Additive Manufacturing 4 (2019), Nr. 4, p. 399–409.

[6] Goldmann, G.: Das Druckerbuch. Technik und Technologien der OCÉ-Drucksysteme (2002), p. 85–90.

[7] Diamond, A. S.; Weiss, D. S.: Handbook of imaging materials. New York: Marcel Dekker (2002).

[8] Weiss, D.; Abkowitz, M.; Kasap, S. et al. (Hrsg.): Handbook of Electronics and Materials. Organic Photoconductors (2017).

[9] Kumar, A.V.; Zhang, H.: Electrophotographic powder deposition for freeform fabrication (1999), p. 1–8.

[10] Boivie, K.; Karlsen, R.; Van der Eijk, C.: Material Issues of the Metal Printing Process, MPP (2006), p. 197–208.

[11] Boivie, K.; Karlsen, R.; Åsebø, O.: The Metal Printing Process; The Development of a New Additive Manufacturing Process for Metallic Materials. Swedish Production Symposium (2008).

[12] Kindermann, P.; Michatz, M., Foerster, J., Anstaett, C.; Seidel, C. et al.: Technological Potential of Electrostatics for Powder Bed Fusion Processes. EuroPM Congress&Exhibition (2019).

[13] Foerster, J. Wunderer, M.; Michatz, M.; et al: Entwicklung eines elektrofotografischen Pulverapplikationsmoduls für laserbasierte Pulverbettschmelzverfahren. Ladungserhalt und Entladung eines Fotoleiters durch Umgebungsbeleuchtung. Rapid.Tech 3D Konferenz (2021).

[14] Binder, M.; Dirnhofer, C.; Kindermann, P. et al.: Procedure and Validation of the Implementation of Automated Sensor Integration Kinematics in an LPBF System. 53rd CIRP Conference on Manufacturing Systems (2019).

[15] Kumar, A.V.; Dutta, A.; Fay, J.E.: Electrophotographic printing of part and binder powders. Rapid Prototyping Journal Vol. 10 (2004), p. 7–13.

[16] Laumer, T.; Stichel, T.; Amend, P. et al.: Simultaneous laser beam melting of multimaterial polymer parts. Journal of Laser Applications Vol. 27 (2014).

[17] Tomas, J.: Mechanische Verfahrenstechnik Schüttgutspeicherung und -transport (2015), p. 369. Internet source: https://kupdf.net/download/mvte6_5af31398e2b6f53b13238784_pdf.

[18] Kuchling, H.: Taschenbuch der Physik. München, Fachbuchverlag Leipzig im Carl Hanser Verlag (2011).

[19] Tipler, P. A.; Mosca, G.; Basler, M.: Physik: Für Wissenschaftler und Ingenieure, (2012).

[20] Tipler, P. A.; Mosca, G.: Diskrete Ladungsverteilung. In: Tipler, P. A.; Mosca, G.; Basler, M.: Physik: Für Wissenschaftler und Ingenieure. Berlin, Springer Spektrum (2012), p. 805–807.